Carpathian Journal of Earth and Environmental Sciences, August 2021, Vol. 16, No. 2, p. 373 – 381; DOI:10.26471/cjees/2021/016/182

THE ORIGIN AND CONTROLLING FACTORS OF SWEET SPOTS IN JURASSIC TIGHT SANDSTONES OF KUQA FORELAND DEPRESSION, TARIM BASIN, NW CHINA

Xianzhang YANG[1,2,3], Dakang ZHONG[1,2] Lu ZHOU[3], Xiaojuan HUANG[1,2], Zhenping XU[3], Yani XIE[3], Guowei ZHANG[3], Xueqi ZHANG[3], Haoyu LUO[3] & Haitao SUN[1,2*]

[1]State Key Laboratory of Petroleum Resources and Prospecting, China University of Petroleum (Beijing), Beijing 102249, China, yangxianzhang@163.com; zhongdakang@263.net
[2]College of Geosciences, China University of Petroleum (Beijing), Beijing, 102249, China,
[3]Tarim Oil Field of CNPC, Xinjiang, 841000, China, e-mail: yangxianzhang@163.com; Tel.: +86 996 2175170
**Corresponding author: haitao.sun@cup.edu.cn; Tel.: +86 10 89733869*

Abstract: Tight sandstone reservoir of Jurassic Ahe Formation in Kuqa depression (Tarim Basin, NW China) has strong heterogeneity, therefore, the prediction of sweet spots is important for natural gas exploration in this area. Based on the collected cores, well logging and seismic data, the detailed analysis of the reservoir space characteristics and origins in the Ahe Formation, the sand body architecture analysis and fractures analysis are carried out to predict the sweet spots. The results of petrologic study shows that the reservoir space of lithic sandstone in the Ahe Formation are intragranular dissolved pores and micro pores, and the area where pores are communicated by effective fractures is easy to form effective reservoir sweet spots. The favorable reservoirs of the Ahe Formation are developed in four types of sand body including progradational bar sandstone, lateral bar sandstone, lag deposits and overflow sand within floodplain. And three types of sweet spots can be predicted by the combination of the sand body and fractures. We believe this research is of great significance to the prediction of sweet spots of tight reservoirs in other foreland basins.

Key words: Kuqa depression, Jurassic, tight sandstone, sand body architecture, sweet spots prediction

1. INTRODUCTION

Tight sandstone gas with low permeability has become important for oil and gas exploration. Industrial gas reservoirs have been found in tight sandstone reservoirs of Yanchang Formation of Upper Triassic in Ordos Basin and Xujiahe formation of Upper Triassic in Sichuan Basin (Sun et al., 2011; Zou et al., 2012; Zhu et al., 2014). The well YN2 in Dibei area of Kuqa depression in Tarim Basin has obtained high-yield gas flow in tight sandstone of Jurassic Ahe Formation. The natural gas resources of Ahe Formation in this area are about 1.23 trillion cubic meters, which is of great exploration potential. However, seven wells have been drilled since then, but only one has achieved high production (Tang et al., 2003; Wang et al., 2013; Yuan et al., 2014; Li et al., 2015; Li et., 2019). The main reason for the failure of other exploration wells is that no sweet spots were found.

Sweet spots are considered to be the area with relatively good porosity and permeability in tight sandstone, which is conducive to the accumulation of natural gas. Furthermore, it is the good tight sandstone reservoir that can provide industrial gas flow (Saigal, et al., 1992; Bjørkum, et al., 1998; Keith et al., 2004; Zhong et al., 2008). Therefore, it is very important to find sweet spots in tight sandstone exploration. Thus, carrying out detailed study on the heterogeneity and sweet spots distribution of tight sandstone reservoirs in the Ahe Formation of Kuqa depression is necessary (Pang et al., 2012; Jiang et al., 2015; Sun et al., 2018; Gao et al., 2020). In this paper, drilling data, outcrop data and seismic data are used to analyze the characteristics and controlling factors of sweet spots in the Ahe Formation, which can improve the prediction of tight sandstone sweet spots in foreland basin.

2. REGIONAL GEOLOGICAL CONDITION

The tight reservoir of Jurassic Ahe Formation in Tarim Basin is developed in the northeast of Kuqa depression (Fig. 1), with a length of 420 km from east to west, a width of 5-20 km from south to north, and an area of 8200 km^2(Ning et al., 2020). Due to strong compression, several high and steep thrust faults in rows are developed in the study area, which is close to the South Tianshan orogenic belt. Dibei area is located in the northeast of Kuqa depression, and the sedimentary system of fault-depressed lacustrine basin is developed in the Jurassic Ahe Formation in this area (Li et al., 2000; Wang et al., 2004; Shen et al., 2005; Wei et al., 2016; Xu et al., 2020). The sedimentary system forms a widely-covered, huge thick sand body with the thickness of 260-300 m. The sand body is mainly composed of lithic sandstone and belongs to low porosity and ultra-low permeability tight reservoir. It forms high-quality natural gas play with overlying mudstone of the Yangxia Formation, and underlying coaly mudstone of the Triassic.

Previous studies on the Jurassic Ahe Formation in Dibei area mainly focused on sedimentary facies types and diagenesis, which mainly included four following points (Wang & Shou, 2001; Tang et al., 2011). First, the Ahe Formation as a whole is developed on a south-dipping monocline, with the main body located at the down-dipping part of the structure. Second, the sandstones of the Ahe Formation are widely distributed, and it is overlaid and directly contacted with the source rocks. Third, the source rocks with coal are well developed, and the vitrinite reflectance is between 0.8% and 2.0%, which is in the stage of gas generation. Sufficient gas source and high-pressure difference between source and reservoir is important guarantee for the formation of tight sandstone gas. Fourth, the sedimentary facies of Jurassic tight reservoir are mainly braided distributary channel and underwater distributary channel sand body of braided river delta. The reservoir is widely distributed with thickness of 100-300 m. The porosity of it is 1.2% - 10.2%, with an average of 6.9%, and the permeability of it is 0.012-84.5mD, with an average of 0.98 mD. Therefore, it is a typical tight reservoir (Wu et al., 2019; Shi et al., 2020).

3. DATA AND METHODS

The data of this paper used include information from outcrops, thin sections and seismic data. Outcrop data is mainly used to analyze faults and fractures. And the width, length and amounts of fractures are measured and counted from the outcrops, which are located in Fig.1. Thin sections are mainly used to analyze the microscopic characteristics of reservoirs. By using polarizing microscope and electronic scanning microscope, core plane porosity is calculated according to point-counting. The ambient voltage of the scanning electron microscope is 20 KV, and the mineral types and contents are obtained by XRD analysis of the cores. Seismic data is provided by CNPC (China National Petroleum Corporation). Horizon calibration and seismic interpretation are carried out by using Landmark software in workstations.

4. PETROLOGY OF TIGHT RESERVOIRS

The main reservoir lithology of Jurassic Ahe Formation in Dibei area is lithic sandstone. The medium-coarse sandstone and conglomeratic sandstone account for 69%. The gravels are mainly composed of quartzite and a small amount of granite. The intergranular fillings are mainly argillaceous matrix, accounting for 4% - 8%, and a little siliceous and calcite cement. The clay minerals of argillaceous matrix are mainly illite, accounting for about 68%, secondly the illite-montmorillonite mixed layers, then the chlorite and kaolinite (Fig. 2). The reservoir is

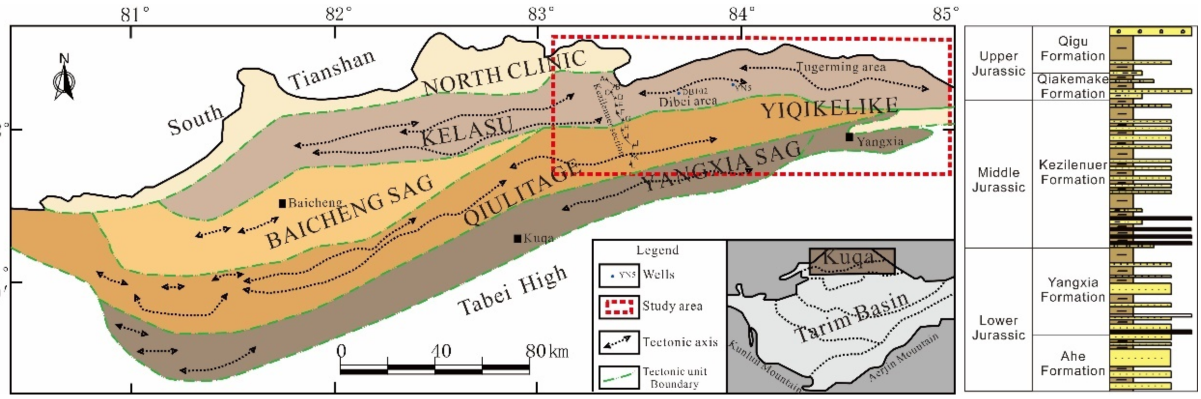

Figure 1. Location of study area in Kuqa Depression of Tarim Basin

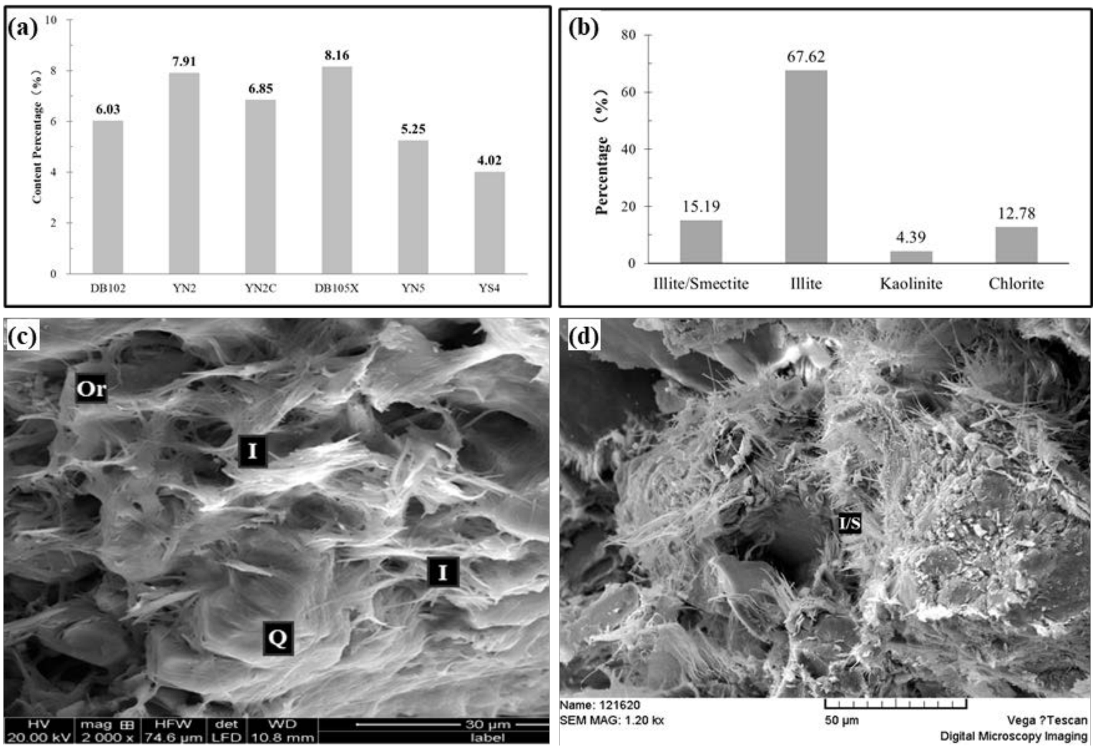

Figure 2. Clay mineral content and SEM characteristics of Jurassic Ahe Formation reservoir
(a), Histogram of absolute content of shale matrix in Jurassic Ahe Formation in Dibei area; (b), Histogram of clay mineral content of Jurassic Ahe Formation reservoir in Dibei area; (c), Well Dibei 105x, J_1a, 4773.43 m, filiform illite; (d) Well Dibei 105x, J_1a, 4773.43 m, filiform illite.

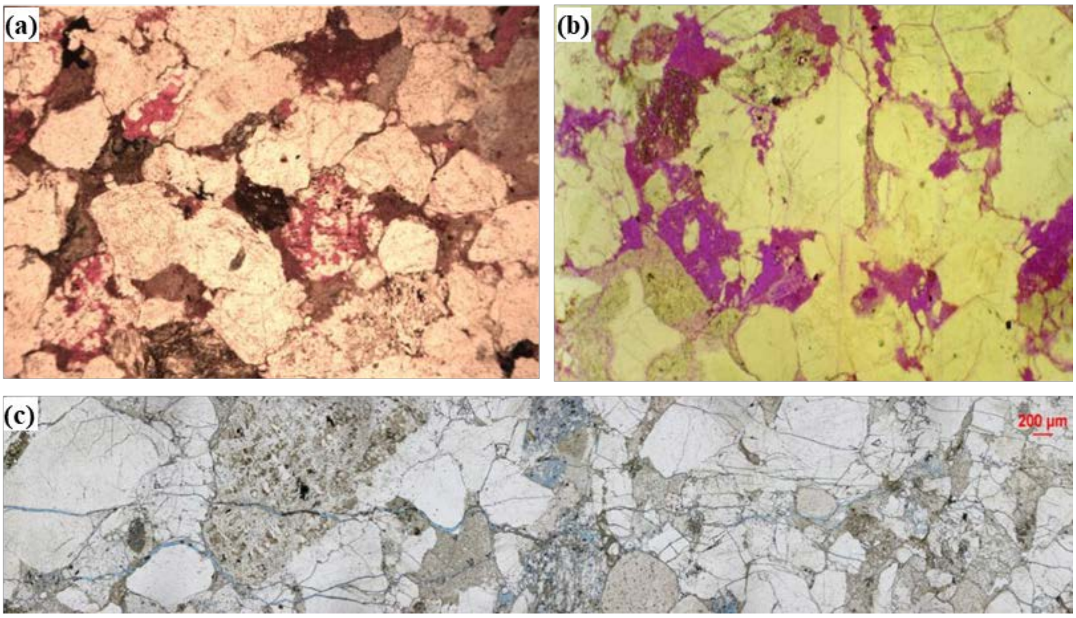

Figure 3. Pore structure characteristics of Jurassic Ahe Formation
(a), Well DiB 102, J_1a, 4935.77 m, with intragranular dissolved pores and micro pores; (b), Well YN4, J_1a, 4376m, intragranular dissolved pores and micro fractures; (c), In well DiB 102, the casting thin section, 5145.21 m, J_1a, the dissolution pores, micro pores and micro fractures are developed;

dominated by intragranular dissolved pores and micro pores, followed by intergranular dissolution enlarged pores. In addition, a large number of micro fractures can be seen on the thin section, which are curved and distributed as a network. The fracture width is mainly distributed in 1-2 μm, effectively connecting the macro pores and micro pores. The pore-throat assembly is mainly micro pore mixed fine throat, and a small amount of large pore mixed fine throat (Fig. 3). The pore coordination number is low, and its average value is less than 3, which means the connectivity between pores is non well. Besides, the mercury removal efficiency is only 30% - 40%. The matrix porosity of the reservoir is mainly distributed in 4% - 12%, with an average of 6.5%. The matrix permeability is mainly distributed in 0.1 - 5 mD, with an average of 0.93 mD. As a whole, the reservoirs are mainly dominated by porous reservoirs with a few in fracture-pore types, belonging to low porosity and ultra-low permeability reservoir.

5. SAND BODY ARCHITECTURE OF TIGHT RESERVOIRS

Previous studies have shown that the sand body of Dibei area are deposited as braided river delta plain (Zhang et al., 2002; Zhang et al., 2011). The multi-stage channels frequently swing and overlap. Therefore, it is necessary to study the sand body architecture and analyze the lithology, grain size and physical properties of different sand bodies (Miall, 1985).

The sandstones of the Ahe Formation are belonging to four types sand body architectures. The size, continuity and physical properties are different from each sand body architectures, which are frequently intersected and overlapped (Fig. 4). Among them, the first type is progradational bar sand, mainly composed of conglomeratic coarse sand and medium sandstone, with plate-shaped cross bedding, trough cross bedding, low angle cross bedding, and other sedimentary structures. The external form is flat bottom and convex up, as the middle to upper part of the channel bar. The primary intergranular pores and intergranular dissolution enlarged pores are main pore types. Intragranular dissolved pores and micropores are also found. Besides, the major throat type is lamellar throat. The physical property of the reservoir is generally good and greater than 9%, meanwhile the longitudinal and transverse permeability between sand bodies is comparatively good. The second type of sand body architecture is lateral bar sand, mainly composed of coarse-fine sandstone and developed trough cross bedding, plate-shaped cross bedding and other sedimentary structures. The external form is tongue shaped, sheet-shaped and lenticular. And the interface form is convex up, belonging to the middle to upper part of distributary channel and the bottom of channel bar. It is dominated by intergranular dissolution enlarged pores. Meanwhile, the intragranular dissolved pores, micropores and micro fractures are also developed. The major throat type is curved lamellar throat, and physical properties of the reservoir are 6%-9%, which is relatively good for reservoirs. But the longitudinal and transverse permeability between sand bodies is relatively poor. The third type of environment is lag deposition, mainly composed of conglomeratic coarse-medium sandstones and small conglomerates, with sedimentary structure of channel cross bedding, plate-shaped cross bedding, scouring structure and graded bedding. The external form is lenticular and the interface form is concave bottom. This kind of reservoir is mainly composed of intragranular dissolved pores, micropores and microfractures. And the major throat type is curved lamellar throat. The physical properties of reservoir are 4% - 6%, which is relatively poor for reservoirs quality. Also, And the longitudinal and transverse permeability between sand bodies is poor. The fourth and the last type of architecture is overflow sand and floodplain, whose lithology is dominated by fine-silty sand, siltstone-mudstone. The sedimentary structures contain laminar bedding, horizontal bedding and wormhole structures. The external form is sheet shape, the interface form is bottom microinvasion. The macro-pores are not connected and developed, mainly developping micro-fractures and micro-pores, and the major throat type is curved lamellar throat. The physical properties of reservoirs are poor, generally less than 4%. The longitudinal and transverse permeability between sand bodies is poor.

In the seismic section (Fig. 5), the Ahe Formation is represented by the 4-5 events or reflections, and each one has a resolution thickness of about 60 m. The internal sand bodies are frequently overlapped vertically and horizontally, and the sand body architecture is complex (Fig. 5). The vertical and horizontal sand body architecture of a single well changes frequently, with distinct reservoir physical properties, poor connectivity and strong heterogeneity. The first and second types of sand body architecture represent 31.9% - 58.8% of the formation thickness. The gas production of single well is related to the sand body thickness of the first kind of architecture. The favorable sand body architecture is the basic condition for the high yield of single well, but not the main control factor. For example, the thickness of the first type architecture in the test section of high-yield well Dixi-1 is only 2.5 m, while that of Yinan-5 and Dibei-102 is 13.5 m and 26.9 m respectively.

6. FAULT-FRACTURE CHARACTERISTICS OF TIGHT RESERVOIR

Due to the influence of tectonic compression stress, faults of large dimension and fractures of small dimension are developed in the sandstone of Jurassic Ahe Formation, connecting the sand layer group and the single sand layer spacious, and being the main control

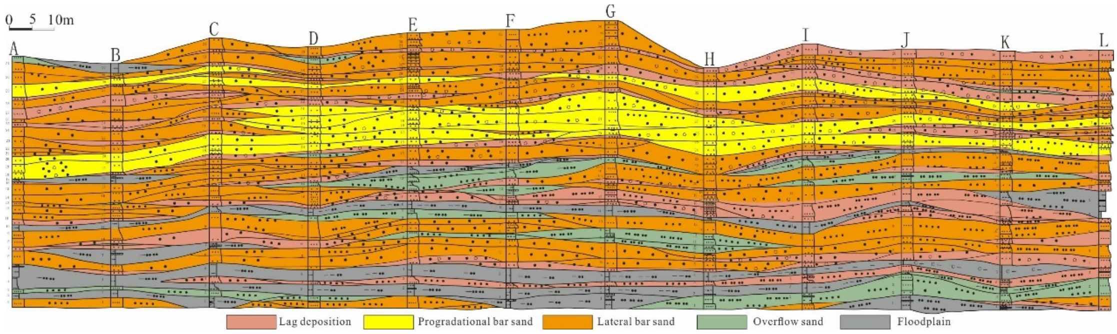

Figure 4. Mesoscale sand body architecture profiles of the first member of Jurassic Ahe Formation in Kezilenuer section.

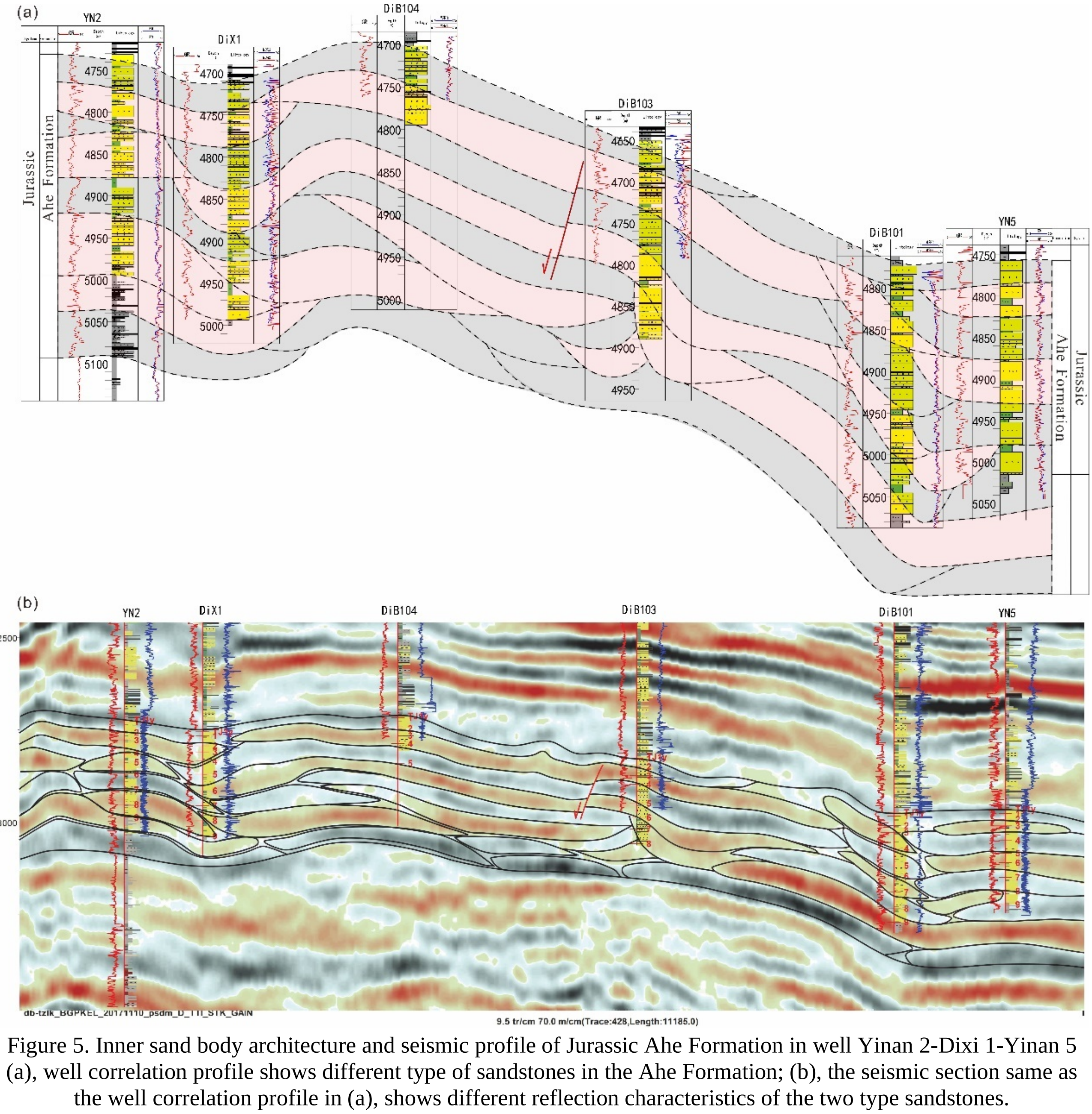

Figure 5. Inner sand body architecture and seismic profile of Jurassic Ahe Formation in well Yinan 2-Dixi 1-Yinan 5 (a), well correlation profile shows different type of sandstones in the Ahe Formation; (b), the seismic section same as the well correlation profile in (a), shows different reflection characteristics of the two type sandstones.

factor for hydrocarbon accumulation and single well production. According to the outcrop observation in the north of Kuqa, some type of faults is controlled by the type of tectonic process like thrusting. The interval of fracture zone is 10-40 m. The width of fracture zone is 30-40 m, and the width / fault distance (k value) is 1.5-1.8. The width of fracture zone controlled by strike slip (or adjustment) fault is 40-150 m, and the width /

fault distance (k value) is 0.13-0.26, which is much smaller than that of thrust fault. According to well core observation, the fractures are mainly tensile or shear. Most of them are curved and unsmooth, with the characters of tensile or shear fractures. They are mostly high angle or straight split fractures, mainly half-filled to unfilled by calcite. The opening is generally 1-2 mm, and the extension length is generally 0.5-1 m. Most fractures are cut off from coal seam and mudstone and high-angle oblique or perpendicular to the strata. According to the interpretation of imaging logging, fractures are mostly high-angle or perpendicular to the strata and develop two groups of strike near E-W and near S-N, with fracture density of 0-0.46 in 1 m. Among them, fractures are most developed in well Dixi-1, Dibei-104 and Tuzi-4 with density of 0.23-0.46 in 1 m. The width of the fracture zone is 10-40 m and the interval of fracture zone is 10-40 m. The degree of fractures development is affected by the thickness and lithology of the strata. The thin layer is more conducive to the development of fractures than the thick layer. And the rock layer is denser the fracture is more favorable to be developped. But the influence of layer thickness on fracture development is obviously greater than the grain size.

Based on seismic profile and drilling data, were identified and interpreted four levels fault-fracture system (Fig. 6) in which first-level, second-level and third-level faults are utilized to interpret conventional profiles, and the four-level fractures are predicted by coherent attributes. First-level faults (F_1), controlling the tectonic boundary, are the thrust fault formed by S-N tectonic compressional stress. The faults are mainly inclined to the north and nearly E-W-striking. The faults disconnect the Neogene, with the fault displacement of 500 m, extending length of more than 20 km and fracture zone of more than 750 m. Second-level faults (F_2), controlling area distribution, are the thrust faults formed by S-N tectonic compressional stress. The faults are mainly inclined to the north, nearly E-W-striking and distributed in echelon form, with the end and end not connected. The faults also disconnect the Jurassic Kezilenuer Formation, with the fault displacement of 150 -500 m, extending length of 10 - 20 km and fracture zone of 225 - 825 m. Third-level faults (F_3), controlling hydrocarbon accumulation, are mainly caused by the regulation in the process of tectonic extrusion and mainly distributed in the tectonic regulation zone. The faults are nearly E-W-striking and also disconnect the Jurassic Ahe Formation, with the fault displacement of 50-150 m, extending length of 1-10 km and fracture zone of 75-225 m. Fourth-level fractures (F_4), controlling high yield of single well, are within the Jurassic Ahe Formation, with the fault displacement of less than 50 m, extending length of less than 1 km. Combining the four levels of fracture-faults causes, regularities of distribution and spatial combination relations, the reservoirs can be divided into three types of fault-fractures combination models (Table. 1). The first combination model is a tensional fracture zone associated with a fold type. The second combination model is a shear fracture zone associated with thrust faults type. The third combination model is a pinnate fracture zones associated with regulated faults.

7. DISCUSSIONS

The main discussions include the following parts:

(1) The sweet spots of the Ahe Formation are controlled by the matching relationship between fracture adjustment zone and sand body architectures.

The tight sandstone reservoir of Ahe Formation is between conventional sandstone and carbonate fracture-pores body. The distribution of geological sweet spots is controlled by four levels of fault-fracture system and high-quality sand body architectures.

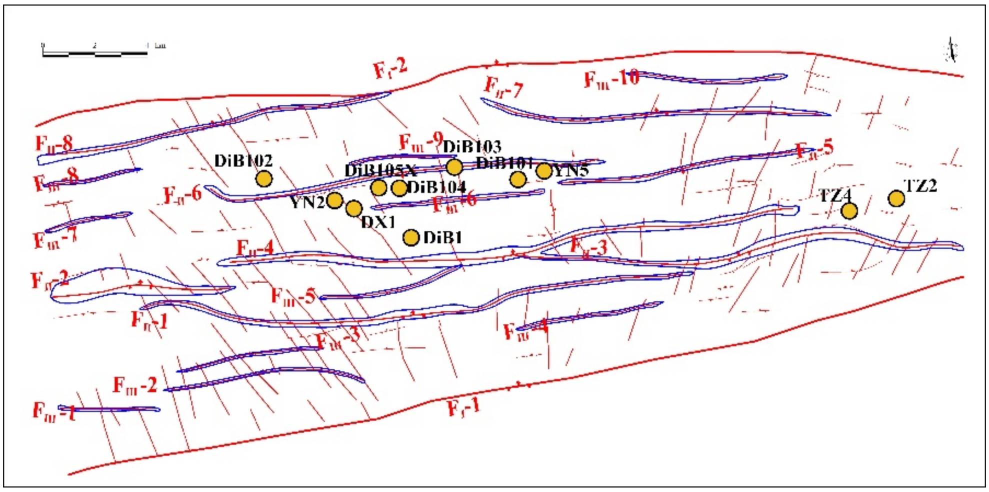

Figure 6. Plane distribution of faults in Jurassic Ahe Formation in Dibei

Table. 1 Three types of fault-fracture combination model of Jurassic Ahe Formation in Dibei

Introduction	Fault types	Outcrops	Seismic section
The tensional fracture zone associated with a fold	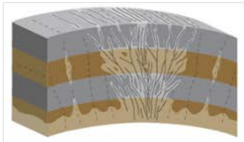		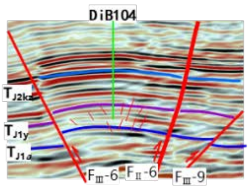
The shear fracture zone associated with thrust faults	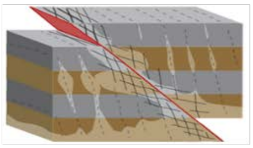		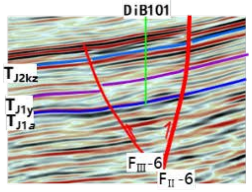
The pinnate fracture zones associated with regulated faults	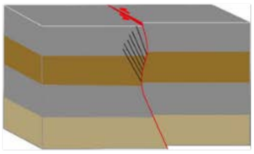		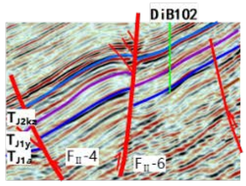

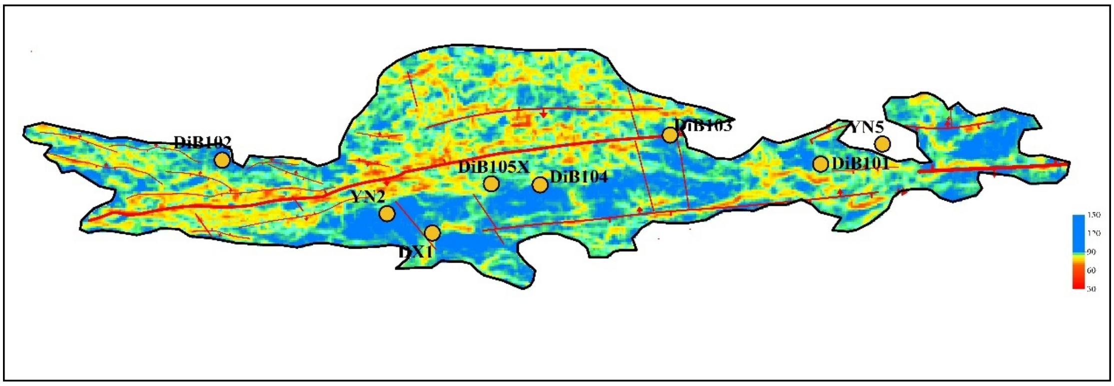

Figure.7 Distribution maps of three types of sweet spots in Jurassic Ahe Formation of Dibei gas reservoirs

According to the fault-fracture combination models, sand body architecture and single well production, three types of sweet spots are divided (Fig. 7). Among them, the first type of sweet spots are the tensional fracture zone and the first/second type sand body development area, and the tensional fractures are mostly high angle oblique or perpendicular to the strata, mainly distributed at the turning point and periphery of tectonic fold recognized into the Dibei 104 and well Dixi-1wells. The second type of sweet spots are shear fracture zone and type I/II architecture sand body development area, and the fractures are mostly high angle oblique or perpendicular to the strata, mainly distributed around the East-West third-level thrust faults, with medium yield of single well and wich meets in the Dibei 101 well. The third type of sweet spots is regulated faults zone and type I/II sand body development area. One part is distributed around the South-North third-level regulated faults with low yield of single well. The typical well where is recognize is Dibei 102, and the other part is distributed around the East-West first-level/second-level faults. The fault zone is used as oil-gas transmission channel, and its peripheral hydrocarbon abundance is low, with low or no production of single well. The typical well is Dibei 103. In addition, the area of no sweet spots and poor fractures has low or no production of single well. The typical well is Yinan 5 with good physical properties of reservoirs. The average porosity and permeability of the well are 9% and 1.46 mD respectively by interpretation of the acoustic and electric logging. The fracture is not developed and with no production in the test.

(2) It is necessary to pay attention to the sensitivity of clay minerals in the Ahe Formation reservoirs during the sweet spots development.

Under the influence of clay minerals, the sensitivity of low porosity and ultra-low permeability reservoirs of pore type in the Ahe Formation with micro pore + fine throat is relatively strong. The sensitivity mainly includes stress sensitivity, water (salt) sensitivity and speed sensitivity. Among them, when the micro fractures are developed and the wall of the fractures is straight and smooth, it is easy to close in the process of oil testing or production, resulting in strong stress sensitivity. The relatively stable mixed layer of illite / montmorillonite is the cause of strong water (salt) sensitivity. And the high content of filamentous illite is the main reason for the high velocity sensitivity. On the Dibei faulted-nose structure, there are 5 wells including Dibei 104, Dixi 1, Dibei 105x, Yinan 2 and Dibei 101. They have similar geological conditions, different drilling fluid systems and different reservoir reconstruction methods, so the production varies greatly. The productivity of nitrogen drilling and nitrogen drilling annulus test in well Dibei 104 and Dixi 1 is high, with a yield of (5.8-8.3)*10^5 m^3/d. And the productivity of the water-based mud drilling and completion acidizing or fracturing test in well Dibei 105x, Yinan 2 and Dibei 101 is middle-low, with a yield ranging from 30,000 m^3/d to 100,000 m^3/d. The study shows that the reservoir of the Ahe Formation generally has strong sensitivity, which affects the production of single well. Therefore, the reservoir protection during the whole production process is needed.

8. CONCLUSIONS

The main conclusion is the next:

(1) The reservoir lithology of Jurassic Ahe Formation is dominated by lithic sandstone, with intragranular dissolved pores, micro-pores and micro-fractures. The interstitial materials are mainly argillaceous matrix, and clay minerals are mainly illite and illite/montmorillonite, which can easily lead to the stronger reservoir sensitivity of the Ahe Formation. The sensitivity mainly includes the stress sensitivity, water (salt) sensitivity and velocity sensitivity.

(2) In the Jurassic Ahe Formation there are four types of sand body architectures. The first type of architecture is progradational bar sand, the second type is lateral bar sand, the third type is lag deposition, and the fourth type is overflow sand and floodplain. Multi-scale faults and fractures, cosmically connecting the sand group and the single sand layer, are the leading factors of controlling hydrocarbon accumulation and single well production. According to the fault-fracture combination models, sand body architectures and single well production, three types of reservoir sweet spots are divided.

REFERENCES

Bjørkum, P.A., Oelkers, E.H., Nadeau, P.H., Walderhaug, O., & Murphy, W.M. 1998, *Porosity prediction in quartzose sandstones as a function of time, temperature, depth, stylolite frequency, and hydrocarbon saturation*. AAPG Bulletin, 82(4): 637–648

Gao Z, Feng J, Cui J, Zhou C, & Shi Y. 2020. *Comparative Analysis on Sedimentary and Reservoir Characteristics of Jurassic to Cretaceous Between Foreland Basins in Southern and Northern Tianshan Mountains*. Xinjiang Petroleum Geology. 41 (1): 80-93.

Jiang Z, Li F, Yang H, Li Z, Liu L, Chen L, & Du Z. 2015. *Development characteristics of fractures in Jurassic tight reservoir in Dibei are of Kuaq depression and its reservoir-controlling factors.* ACTA Petrolei Sinica, 36(S2): 102－111.

Keith W, Robert M, & John W. 2004. *Factors controlling prolific gas production from low －permeability sandstone reservoirs: Implications for resource assessment, prospect development, and risk analysis*. AAPG Bulletin. 88: 1083－1121.

Li F, Jiang Z, Li Z, Wang X, Du Z, Luo S, & Xin S. 2015. *Enriched mechanism of natural gas of Lower Jurssic in Dibei area, Kuqa depression*. Earth Science-Journal of China University of Geoscieces. 40(09): 1538－1548.

Li J, Wang C, Li J, Ma W, Zhang H, Lu Y, Li D, & Liu M. 2019. *Source and exploration direction of tight oil and gas in the Dibei section of northern Kuqa depression*. China Petroleum Exploration, 24(04):87-99.

Li W, Wang C, & Gao Z. 2000. *Sedimentary evolution of Mesozoic Era in Kuche depression, Tarim Basin*. Acta Sedimentologica Sinica.18(4): 534-538.

Miall A D. 1985. *Architectural-Element Analysis: A New Method of Facies Analysis Applied to Fluvial Deposits*. Earth Science Reviews. 22: 261-308.

Ning F, Mao G, Yun J, Zhang Z, & Dong L. 2020. *Differential interlayer deformation and its significance for hydrocarbon accumulation in the Tazhong area, Tarim Basin, nw China*. Carpathian Journal of Earth and Environmental Sciences. 15(1):113-125.

Pang X, Zhou X, Jiang Z, Wang Z, Li S, Tian J, Xiang C, Yang H, Chen D, Yang W & Pang H. 2012. *Hydrocarbon reservoirs formation, evolution, prediction and evaluation in the superimposed Basins*. ACTA Geologica Sinica, 86(1), 1-103.

Saigal G, Bjørkum P, & Larter S. 1992, *The effects of oil emplacement in diagenetic processes—Examples from the Fulmar reservoir sandstones: Central North Sea*. AAPG Bulletin, 76(7), 1024-1033.

Shen Y, Wu C, Yue L. & Xie X. 2005. *An analysis of Jurassic sandstone fragment components and their provenance in Kuqa depression*. ACTA Geoscientica Sinica.26(03): 235－240.

Shi C, Xu A, Wei H, Hu C, Zhang X, Zhang W, Mo T,

Zhang H, Zhou L, Shi L, Zhu W, & Chen W. 2020. *Quantitative characterization on the clastic reservoir destruction by tectonic compression: a case study of the Jurassic Ahe Formation in Yiqikelike structural belt, Kuqa depression*. ACTA Petrolei Sinica, 41(2): 205-216.

Sun H, Zhong D, Zhang X, & Liu H. 2011. *Characteristics and mechanism of Permian Shanxi tight reservoir of Changbei gas field,Ordos Basin* . ACTA Sedimentologica Sinica,(04): 724－733.

Sun, H, Zhong, D, Li, Y, Mao Y, Yang X, & Zhang C. 2018, *Porosity origin and controlling factors of ultra-deep sandstones reservoirs with low porosity and ultra-low permeability: a case of Bashijiqike Formation in Keshen area of Kuqa Depression, Tarim Basin, NW China*. Journal of Jilin University, Earth Science. Edition. 48, 693-704.

Tang H, Wang G, Peng S, Wang Y, Qian L, & Lu Y. 2003. *Exploration prospects for natural gas in Kuqa Depression*. Natural Gas Geoscience. 2003(06): 459-462.

Tang Y, Luo J, Ma Y, Yang X, Ye M, & He Q. 2011. *Effect of Alkaline Diagenetic Environment of Lower Jurassic on Reservoir Property in Kuqa Depression*. Xinjiang Petroleum Geology, 32(04): 356－358.

Wang G, & Shou J. 2001. *The relationship between the characteristics of sand bodies and the properties of Lower Jurassic reservoirs in eastern Kuqa depression, Tarim Basin.* Petroleum Exploration and Development. 28(04): 33－35.

Wang Q, Yang M, & Lv X. 2004. *Features of structural segmentation and accumulation of oil and gas in the Qiulitage structural belt, Kuqa fold and thrust belt*. Chinese Journal of Geology, 39(04):523-531.

Wang Z, Xie H, Li Y, Lei G, Wu C, Yang X, Ma Y. & Neng Y. 2013. *Exploration and discovery of large and deep subsalt gas fields in Kuqa foreland thrust belt*. China Petroleum Exploration, 18(3): 1-11.

Wei H, Huang W, Luo H, Li L, Shi L. & Wang Z. 2016. *Faults characteristics and evolution in the eastern Kuqa depression*. Earth Science. 41(06): 1074－1080.

Wu J, Wang B, Zhu C, Gong Q, Song G. & Wang H. 2019. *Influences of Feldspar Dissolution on Reservoir Physical Properties of Clastics in the Lower Jurassic Coal Measures, Eastern Kuqa Depression*. Xinjiang Petroleum Geology. 40(06): 649－657.

Xu X, Wang C, Liu M, Lin S, Li D. & Gao Z. 2020. *Provenance characteristics of Upper Triassic-Middle Jurassic in the eastern Kuqa depression of Tarim Basin, China and their geological significance*. Journal of Earth Sciences and Environment, 42(02):172-187.

Yuan W, Wang P, Qin H, Pang X, Zhang B, Du Z. & Xing X. 2014. *Accumulation conditions for the continuous tight-sandstone gas in Jurassic, Kuqa depression*. Journal of Northeast Petroleum Univeristy, 38(04): 1－10.

Zhang G, Ma Y, Han W. & Luo J. 2011. *Provenance analysis of the Early －Middle Jurassic deposits in eastern Kuqa depression in the Tarim Basin，Xinjiang*. Sedimentary Geology and Tethyan Geology, 31(03): 39－46.

Zhang H, Shou J, Chen Z, Wang S, Yang X, Pi X, & Cai Z. 2002. *Sedimentary characterisitcs and sandstone body distribution of the Lower Jurassic in Kuqa depression*. Journal of Palaeogeography. 4(03): 47-58.

Zhong D, Zhu X, & Wang H. 2008. *Characteristic and formation mechanism of deep buried clastic reservoir*. Science in China: Series D. 38(S1), 11-18.

Zou C, Zhu, R, Wu S, Yang Z, Tao S, Yuan X, Hou L, Yang H, Xu C, & Li S. 2012. *Types, characteristics, genesis and prospect of conventional and unconventional hydrocarbon accumulations: taking tight oil and tight gas in China as an instance*. ACTA Petrolei Sinica. 33(02): 173－187.

Zhu H, Zhong D，Zhang Y, Sun H, & Yang Z． 2014. *Pore types and controlling factors on porosity and permeability of Upper Triassic Xujiahe tight sandstone reservoir in Southern Sichuan Basin*. Oil ＆ Gas Geology, 35(1): 65－76．

Received at: 03. 03. 2021
Revised at: 07. 06. 2021
Accepted for publication at: 21. 06. 2021
Published online at: 26. 06. 2021